



Lanthanide coordination polymers based on multi-donor ligand containing pyridine and phthalate moieties: Structures, luminescence and magnetic properties



Xun Feng ^a, Lang Liu ^{c,a}, Li-Ya Wang ^{a,b,*}, Hong-Liang Song ^a, Zhi Qiang Shi ^a, Xu-Hong Wu ^a, Seik-Weng Ng ^{d,e}

^a College of Chemistry and Chemical Engineering, Luoyang Normal University, Luoyang 471022, PR China

^b College of Chemistry and Pharmacy Engineering, Nanyang Normal University, Nanyang 473601, PR China

^c College of Chemistry and Molecular Engineering, Zhengzhou University, Zhengzhou 450002, PR China

^d Department of Chemistry, University of Malaya, Kuala Lumpur 50603, Malaysia

^e Chemistry Department, Faculty of Science, King Abdulaziz University, Jeddah 80203, Saudi Arabia

ARTICLE INFO

Article history:

Received 15 June 2013

Received in revised form

8 August 2013

Accepted 24 August 2013

Available online 5 September 2013

Keywords:

Lanthanide coordination polymer

Single crystal structure

Luminescence

Magnetic properties

ABSTRACT

A new family of five lanthanide-organic coordination polymers incorporating multi-functional N-heterocyclic dicarboxylate ligand, namely, $[Ln_2(Hdpp)_2(dpp)_2]_n$, $Ln=Pr(\mathbf{1})$, $Eu(\mathbf{2})$, $Gd(\mathbf{3})$, $Dy(\mathbf{4})$, $Er(\mathbf{5})$ ($H_2dpp=1-(3,4\text{-dicarboxyphenyl})\text{-pyridin-4-ol}$) have been fabricated successfully through solvothermal reaction of 1-(3,4-dicarboxyphenyl)-4-hydroxypyridin-1-iun chloride with trivalent lanthanide salts, and have been characterized systematically. The complexes 1–5 are isomorphous and isostructural. They all feature three dimensional (3D) frameworks based on the interconnection of 1D double chains composed of the binuclear moiety $[Ln_2(Hdpp)_2]^{4+}$ basic carboxylate as secondary building unit (SBU). The results of magnetic analysis shows the same bridging fashion of carboxylic group in this case results in the different magnetic properties occurring within lanthanide polymers. Moreover, the Eu(III) and Dy(III) complexes display characteristic luminescence emission in the visible regions.

© 2013 Elsevier Inc. All rights reserved.

1. Introduction

The design and construction of lanthanide-metal-organic frameworks (Ln-MOFs) based on the judicious selection of ligands and metal ions have become a very attractive research field of coordination chemistry and crystal engineering. The motive comes not only from their fascinating architectures and topologies, but also from the demand for applications of functional materials in the field of catalysis, magnetism, luminescence, sensing, nonlinear optics and medical imaging reagents [1]. It is well known that trivalent lanthanide ions are fascinating luminescence sources for their high color purity and relatively long lifetimes arising from electronic transitions within the partially filled 4f-shell [2]. Lanthanide luminescence in organometallic complexes is typically accomplished by the use of antenna linkers [3], because it can efficiently transfer the energy gained through photon absorption to the lanthanide ions in the complexes [4]. Over the last decades, a variety of multi-carboxylate imidazoline/pyridine-based ligands have been extensively employed for construction of functional MOF [5]. However, to the best of our knowledge, lanthanide metal compounds constructed from the multi-donor system containing both

pyridine and phthalate moiety have seldom been reported, the photoluminescent and magnetic properties are still badly understood [6]. This ligand including hydroxyl and carboxylic group is expected to exhibit various bridging features, due to its abilities and strong coordination tendency to high dimensional robust networks, exhibiting tunable ferro or antiferro-magnetic exchanges in complexes [7,8]. As a contribution to the elucidation of structures of lanthanide carboxylates, as well as better understand the nature of the physical property in these systems, we present herein the syntheses, structures, photoluminescence, and magnetic properties of a family lanthanide-organic frameworks based on flexible multi-oxygen donor N-heterocyclic ligand. It is hoped that combination of two types of ligands will enhance the energy-transfer efficiency from ligand to lanthanide (III) ions [9]. Meanwhile, utilization of heavy lanthanide ions such as Dy (III), Er(III) also become more popular in the design and synthesis of single molecule magnets due to their larger angular moment and strong magnetic anisotropy in the ground multiple states [10].

2. Experimental

2.1. Materials and physical measurements

All reagents used in the syntheses were of analytical grade and used as received from Jinan Camolai Trading Company of China.

* Corresponding author at: College of Chemistry and Chemical Engineering, Luoyang Normal University, Luoyang 471022, China. Tel.: +86 379 6552 3593; fax: +86 379 6551 1205.

E-mail address: wlya@lynu.edu.cn (L.-Y. Wang).

Table 1

Crystal data and structure refinement for complexes 1–5.

Compounds No.	1	2	3	4	5
Empirical formula	C ₂₆ H ₁₅ N ₂ O ₁₀ Pr	C ₂₆ H ₁₅ N ₂ O ₁₀ Eu	C ₂₆ H ₁₅ N ₂ O ₁₀ Gd	C ₂₆ H ₁₅ N ₂ O ₁₀ Dy	C ₂₆ H ₁₅ N ₂ O ₁₀ Er
Formula weight	656.31	667.36	672.65	677.90	682.66
Temperature	296(2)	293(2)	296(2)	293(2)	293(2)
Crystal system	Triclinic	Triclinic	Triclinic	Triclinic	Triclinic
Space group	P–1	P–1	P–1	P–1	P–1
Unit cell dimensions (Å, deg)	a=7.740(4) b=10.758(6) c=14.417(8) α=75.259(7) β=84.233(8) γ=75.742(7)	a=7.6625(8) b=10.6656(11) c=14.3777(15) α=75.587(1) β=84.551(1) γ=75.942(1)	a=7.644(3) b=10.634(4) c=14.374(5) α=75.506(5) β=84.422(6) γ=75.941(5)	a=7.627(2) b=10.595(3) c=14.368(4) α=75.900(4) β=84.592(4) γ=75.795(4)	a=7.6350(4) b=10.6255(5) c=14.3727(8) α=75.6702(7) β=84.5632(8) γ=75.8766(7)
Volume (Å ³), Z	1124.4(10), 2	1103.2(2), 2	1096.5(7), 2	1091.0(5), 2	1094.84(10), 2
Calculated density (g/cm ³)	1.939	2.009	2.037	2.064	2.071
F(000)	648	656	658	662	666
Crystal size (mm ³)	0.24 × 0.18 × 0.14	0.19 × 0.18 × 0.16	0.23 × 0.18 × 0.14	0.35 × 0.26 × 0.17	0.36 × 0.23 × 0.18
Refls. total	6300	6601	5823	6199	6760
Refls. unique	4501	4720	4032	4377	4878
Refls. observed	4326	4552	3743	4108	4657
Absorption coefficient	2.236	2.914	3.096	3.496	3.904
Goodness of fit (GOF)	1.008	1.047	1.022	1.001	1.017
Final R indices [<i>I</i> > 2σ(<i>I</i>)] ^a	R ₁ =0.0275, wR ₂ =0.0779	R ₁ =0.0202, wR ₂ =0.0510	R ₁ =0.0227, wR ₂ =0.0585	R ₁ =0.0208, wR ₂ =0.0499	R ₁ =0.0244, wR ₂ =0.0678
R indices (all data) ^a	R ₁ =0.0285, wR ₂ =0.0789	R ₁ =0.0210, wR ₂ =0.0514	R ₁ =0.0254, wR ₂ =0.0602	R ₁ =0.0230, wR ₂ =0.051	R ₁ =0.0257, wR ₂ =0.0689
Largest diff. peak and hole (e Å ^{−3})	1.068 and –1.616	0.765 and –1.024	0.600 and –0.860	0.665 and –0.736	1.278 and –1.392

$$R = \sum |F_0| - |F_c| / \sum |F_0|, wR = \{ \sum [w(F_0^2 - F_c^2)^2] / \sum (F_0^2)^2 \}^{1/2}.$$

Elemental analyses for carbon, hydrogen and nitrogen atoms were performed on a Vario EL III elemental analyzer. The infrared spectra (4000–400 cm^{−1}) were recorded by using KBr pellet on an AvatarTM 360 E. S. P. IR spectrometer. Luminescence spectra of the complexes in solid state were run on a Cary Eclipse fluorescence spectrophotometer. Variable-temperature magnetic susceptibilities were measured using a MPMS-7 SQUID magnetometer under a 0.2 T applied magnetic field and over the range of 2–300 K. Diamagnetic corrections were made with Pascal's constants for all constituent atoms.

2.2. Syntheses of the complexes

[Ln₂(Hdpp)₂(dpp)₂]_n (*Ln*=Pr(**1**), Eu(**2**), Gd(**3**), Dy(**4**), Er(**5**)): an zwitter organic compound 1-(3,4-dicarboxyphenyl)-4-hydroxypyridin-1-iun chloride (0.061 g, 0.2 mmol) and sodium formate dihydrate (0.020 g, 0.15 mmol) in a solution of water/alcohol (v/v=1.5, 10 mL) were mixed with an aqueous solution (10 mL) of 0.1 mmol lanthanide(III) nitrate hexahydrate, ((**1**)=Pr(NO₃)₃·6H₂O, 0.041 g; (**2**)=Eu(NO₃)₃·6H₂O, 0.043 g, (**3**)=Gd(NO₃)₃·6H₂O, 0.045 g, (**4**)=Dy(NO₃)₃·6H₂O, 0.046 g, (**5**)=Er(NO₃)₃·6H₂O, 0.047 g). After stirring for 20 min in air, the pH value was adjusted to 3.0 with nitric acid, and the mixture was placed into 25 mL Teflon-lined autoclave under autogenous pressure being heated at 155 °C for 72 h, then the autoclave was cooled over a period of 24 h at a rate 5 °C/h. After filtration, the product was washed with distilled water and then dried, green crystals of **1** were obtained suitable for X-ray diffraction analysis. For (**1**), yield: 0.0282 g (43%) based on lanthanide element. Elemental analysis (%): calcd for C₂₆H₁₅N₂O₁₀Pr: C 47.58, H 2.30, N 4.27, found: C 47.62, H 2.26, N 4.23. IR (KBr pellet, cm^{−1}): 3389s, 2278s, 1607s, 1559s, 1472s, 1333m, 1279s, 1112s, 866m, 793 s, 660s, 519s. For (**2**), yield: 0.0292 g (44%). Elemental analysis (%): calcd. for C₂₆H₁₅N₂O₁₀Eu: C 46.79, H 2.26, N 4.19, found: C 46.53, H 2.19, N 4.18. IR (KBr pellet, cm^{−1}): 3402s, 3122br, 1623s, 1532s, 1413m, 1374s, 1087s, 929vs, 747m, 660s. For (**3**), yield: 0.0264 g (39%). Elemental analysis (%): calcd. for C₂₆H₁₅N₂O₁₀Gd: C 46.42, H, 2.24, N 4.16, found: C 46.27, H 2.18, N 4.13. IR (KBr pellet, cm^{−1}): 3420vs, 1626vs, 1612s, 1442s, 1392s, 1279s, 1068s, 1012vs, 832s,

763s. For (**4**), yield: 0.0296 g (45%). Elemental analysis (%): calcd. for C₂₆H₁₅N₂O₁₀Dy: C 46.06, H, 2.23, N 4.13. found: C 46.13, H 2.28, N 4.21. IR (KBr pellet, cm^{−1}): 3420vs, 1784s, 1626vs, 1612s, 1442s, 1392s, 1319m, 1279s, 1068s, 1012vs, 832s, 810m, 663s. For (**5**), yield: 0.0281 g (41%). Elemental analysis (%): calcd. for C₂₆H₁₅N₂O₁₀Er: C 45.90, H, 2.22, N 4.11, found: C 45.71, H 2.28, N 4.27. IR (KBr pellet, cm^{−1}): 3390vs, 1784s, 1626vs, 1612s, 1442s, 1392s, 1319m, 1279s, 1068s, 1012vs, 832s, 743s, 623m.

2.3. Crystallographic data collection and refinement

Single-crystal diffraction data of **1**–**5** were collected on a Bruker SMART APEX CCD diffractometer with graphite-monochromated MoKα radiation ($\lambda=0.71073$ Å) at room temperature. The structures were solved using direct methods and successive Fourier difference synthesis (SHELXS-97) [11](a), and refined using the full-matrix least-squares method on *F*² with anisotropic thermal parameters for all non-hydrogen atoms (SHELXL-97) [11](b). An empirical absorption correction was applied using the SADABS program. The hydrogen atoms of organic ligands were placed in calculated positions and refined using a riding on attached atoms with isotropic thermal parameters 1.2 times those of their carrier atoms. The water hydrogen atoms were located from difference maps and refined with isotropic thermal parameters 1.5 times those of their carrier atoms. The summary crystallographic data and selected bond lengths and angles, hydrogen bonding parameters for **1**–**5** are listed in Table 1 and Tables S1, S2 Supplementary material, respectively.

3. Results and discussion

3.1. Single-crystal structure determination

3.1.1. [Ln₂(Hdpp)₂(dpp)₂]_n (*Ln*=Pr(**1**), Eu(**2**), Gd(**3**), Dy(**4**), Er(**5**))

Single X-ray diffraction analyses reveal that compounds **1**–**5** are isomorphous and isostructural, all they crystallize in triclinic system with space group of *P*–1, featuring 3D conuent frameworks based

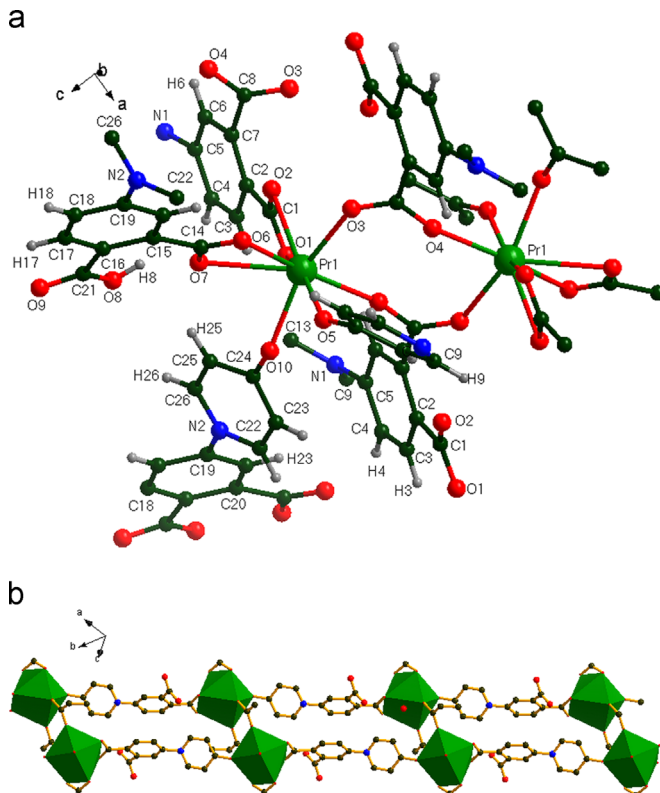


Fig. 1. (a) The coordination environment of Pr(III) ion in the symmetry unit of **1** viewed along *ac* plane. (b) Polyhedral diagram of the 1D double-stranded chains of Pr(1) ions linked by the full deprotonated dpp²⁻ ligand viewed approximately down *b*-axis in **1**.

on 1D double-stranded lanthanide-carboxylate motifs. Therefore, structure of **1** was selected and described in details to represent their frameworks. As illustrated in Fig. 1a, the symmetric unit of **1** contains two crystallographically independent Pr(III) cations and four H₂dpp ligands, whereas the fromate anion does not present in the final product. Interestingly, there are no solvent or crystallization water molecules, even without coordinated terminal aqueous ligand in the structure, which proves that it is crystallized from an ethanol–water aqueous medium. Presumably the abundance of coordination sites and chelating ability of the mixed donor ligand preclude the possibility of water binding to central *Ln*(III) ion, and this restriction of O–H vibrational resonance always enhances the luminescence of the given lanthanoid [12]. The Pr(III) ion is eight coordinated bonding six H₂dpp anion ligands. The extremely distorted dodecahedral geometry Pr{O₈} around the central ion is completed by eight O atoms, of which six carboxylate O atoms are from two distinct carboxylic groups and two O atoms are from hydroxyl pyridine moieties of two independent Hdpp[−] ligands. The Pr1–O bond lengths fall in the range of 2.358(2)–2.730(3) Å, with an average value of ca. 2.439 Å for octa-coordinated Pr(1) ions (see Table S1). This is closely related to those observed for other Pr(III) complexes with similar amino acid-like ligands [13]. Among the six multi-carboxylic ligands, four are completely deprotonated, while the other two just are partially deprotonated, being denoted as dpp^{2−} and Hdpp[−] respectively. It is interesting that both two kinds of ligand adopt the chelating and bi-monodentate bridging fashions, linking neighboring Pr(III) ion (see Scheme 1(a)). Two adjacent Pr(III) ions are doubly bridged by two carboxylic groups from Hdpp[−], exhibiting a cyclooctane-like configuration, as indicated in Fig. S1, Supporting materials. The two Pr(III) metal units are exactly identical, making the molecule symmetry with an inversion symmetry center, each. This binuclear array can be

compared with those of homodinuclear lanthanide xanthene-9-carboxylate complexes [14].

The binuclear unit is between outer benzene rings, giving an arborization-like array, however, the pyridine and phenyl ring are not coplanar. The dihedral angles between pyridine and phenyl ring within the same Hdpp[−] ligand is 48.83°, while the dihedral angles between two phenyl rings sharing the common Pr(III) ion are 71.26°, and the carboxyl group is nearly in the plane of benzene ring. The second category of ligand is fully deprotonated, acting as a penta-dentate ligand. This entangled ligand displays μ₄-kO, O': kO: k O: kO' fashion to link four adjacent Pr(III) ions. Both two carboxylic groups of dpp^{2−} adopt the bis-(bridging) bidentate as well as monodentate modes (see Scheme 1(b)). While, each Hdpp[−] ligand employs the 3-carboxylate group oxygen to chelate another Pr(1) ion and using 4-hydroxyl oxygen connect the third Pr(1) ion. The two neighboring Pr(1) ions are double linked via 3-carboxylate group to form a Pr₂ binuclear unit with the Pr · · · Pr separation of 5.522 Å. These dinuclear segments are grafted on to the infinite 1D double-stranded chain arrays along the crystallographic *c*-axis through the carboxylate oxygen atoms from phthalate moiety and oxygen atoms derived from the hydroxyl-pyridine entity, as shown in Fig. 1b, and projection view along *ab* plane is shown in Fig. S3, Supporting materials. The nearest Pr · · · Pr separation within this chain is 6.586 Å. Meantime, Hdpp[−] ligand acts as a linker using the 3-carboxylate oxygen, consequently interconnects these 1-D chains into a 2D corrugated grid along *a*-axis, as displayed in Fig. 2a, in which the adjacent binuclear units are linked together by the μ₂-O bridging from 4-carboxylate group of the Hdpp[−] ligand to generate a parallelogram aggregate composed of four neighboring Pr(1) ions, and the diagonal-to-diagonal distances are 12.41, 10.34 Å, respectively (see Fig. 1b). The individual nets are lattice in nature, and the rhombus 4, 4 order topology layers arises [15]. Moreover the puckered chain connected by Hdpp[−], covers and reinforces this 2D sheet from upside, as shown in Fig. 2b, but this does not result in interpenetrating formation. The coordination modes of the ligand are essentially different from that of divalent zinc and cadmium coordination polymers containing analogs flexible ligand [16], in which, two carboxylate groups have a dihedral angle of 14.8° and 86.5° toward the plane of the corresponding phenyl rings. The combination of the pyridine ring and phenyl ring are twisted across the C–N bond and these twisted carboxylate groups result in the formation of (Cd–L)_n and (Cd–PA)_n helical chains.

These 2D layers are further interconnected and extended through terminal oxygen atoms from carboxylate and hydroxyl pyridine, into a 3D convient complicated coordination networks consequently, as demonstrated in Fig. 3a. The distance between the adjacent layers is 13.309 Å. This array can be comparable to the series of lanthanide coordination polymers containing the 2,2'-bipyridyl-4,4'-dicarboxylic acid with the similar crystal system [17]. Packing view of the 3D structure along *b c* plane projection is shown in Fig. S3, in Supporting materials. The hydrogen bonding (see Fig. S4 and Tab S2) and π–π stacking interactions are also observed.

A better insight into the nature of this framework can be achieved by the application of a topological approach, i.e. reducing the multidimensional structures to simple node and connecting nets. The dpp^{2−} bridged dinuclear Pr(III) unit was treated as one node, producing a 4, 4-connected net square lattice topology (Fig. 2a). Then the ligand further interconnected these 2D sheet via carboxylic O and phenolic-hydroxyl O into a (4, 6)-connected 3D framework. The total Schläfli symbol is (4³5²6)(4³5⁶6⁷). [18] as illustrated in Fig. 3b. It should be pointed out that in present work from the light lanthanide praseodymium complex of **1** to the heavy lanthanide erbium complex **5**, they all exhibit the same 3D lattice array. This case is different from those lanthanide coordination polymers based on the multi-N, O-donor ligands

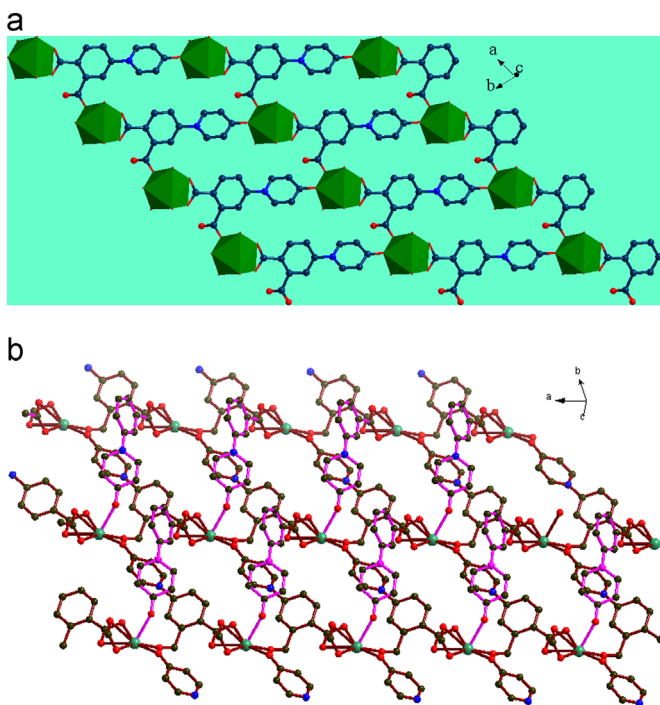


Fig. 2. (a) Polyhedral view of the monolayer 2-D layers with homo-rectangle windows in **1** along *ab* plane. Color codes: sea green, Pr; blue, N; red, O; black, C, the H atoms are not included for clarity. (b) Diamond illustration of the individual $[\text{Pr}(\text{dpp})]^+$ layer (black) covered by Hdpp^- from upside, viewed approximately down *bc* plane in **1**. The reader is referred to the web version of this article. (For interpretation of the references to color in this figure legend, the reader is referred to the web version of this article.)

previous reported, which exhibit diverse structures [19],[5](f),[7] (c),[8](c),[15](a). However, similarities in bonding motifs for the series of lanthanide complexes allow us to compare the metal-donor bond distances in the same array. Table S1 in Supporting materials, compares the average bond distances for the Ln–O and metal···metal distances, which could only be compared for complexes that exhibit the same arrays. As the ionic radius of the metal become smaller in the order Pr(III)>Eu(III)>Gd(III)>Dy(III)>Er(III), their corresponding bond lengths decrease, consistent with the lanthanide contraction effect. In addition, comparative investigation on the isostructural complexes **1–5** have found that in the same 1D chain (see Fig. S2, Supplementary material), the $\text{Ln}(1)\cdots\text{Ln}(1)$ separations double bridged by carboxylic group also display their decrease trend with increasing of elements order, which are also consistent with the lanthanide contraction [20], as listed in Table 2 for details.

3.2. PXRD measurements and analysis

The purity and homogeneity of the bulk products of **1–5** were measured and determined by comparison of the simulated and experimental X-ray powder diffraction patterns. As depicted in Figs. 4 and S5–S8, Supplementary material. The peak positions of the experimental patterns for these complexes (of the final bulk material) are nearly identical to those of corresponding simulated ones generated from single-crystal X-ray diffraction data, although some minor Bragg peak positions have been shifted in comparison to the simulated ones.

3.3. Photoluminescence properties

The photoluminescence properties of the solid powder samples of **1–5**, as well as free H₂dpp ligand samples were investigated at

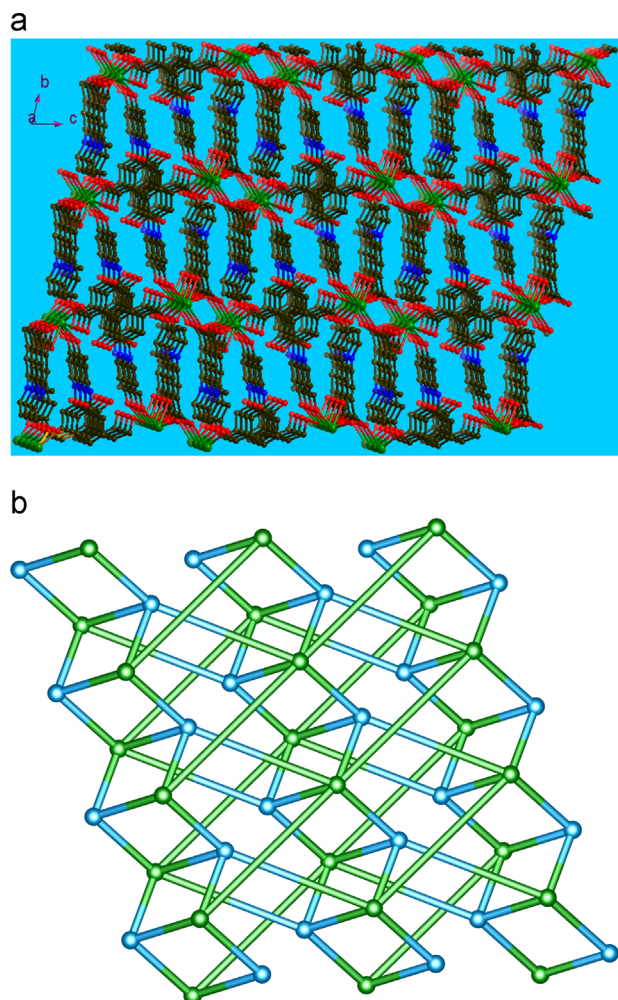


Fig. 3. (a) Projective view of the 3D packing structure of **1** showing 1D open channels connected by Hdpp^- ligands along the *a*-axis. (All hydrogen atoms are omitted for clarity. Pr(1) is presented by the green ball.) (b) Schematic illustrating the 3-D network with a binodal (4, 6)-connected topology for **1**. (The azure and green balls represented two kinds of Pr(1) nodes.) (For interpretation of the references to color in this figure legend, the reader is referred to the web version of this article.)

Table 2

Comparing of bond length and $\text{Ln}\cdots\text{Ln}$ separations for series of complexes.

Complex	Average bond distances of $\text{Ln}-\text{O}$ (\AA)	Separation of $\text{Ln}(1)\cdots\text{Ln}(1)$ bridged via Hdpp (\AA)
1 (Pr)	2.484	5.522
2 (Eu)	2.428	5.495
3 (Gd)	2.417	5.475
4 (Dy)	2.401	5.453
5 (Er)	2.398	5.446

room temperature, and the results as reported in Figs. 5–7 and Fig. S9, Supplementary material, respectively. As indicated in Fig. S9, the excitation spectrum of free ligand shows a broad band at 356 nm (monitored at emission wavelength of ca 450 nm), which is attributed to the $\pi-\pi^*$ transition of the aromatic/pyridine ring chromophores [21]. Upon photoexcitation with 360 nm, the emission spectrum of H₃dpp ligand presents a large broad band with $\lambda_{max}=427$ nm, presumably because of excited-state intramolecular proton transfer (ESIPT) from the hydroxyl group to the nearby carbonyl moiety of the H₂dpp ligand. This type of ESIPT is known to occur in Schiff base and p-methoxy substituted salicylates, with similar excitation and emission wavelengths [22].

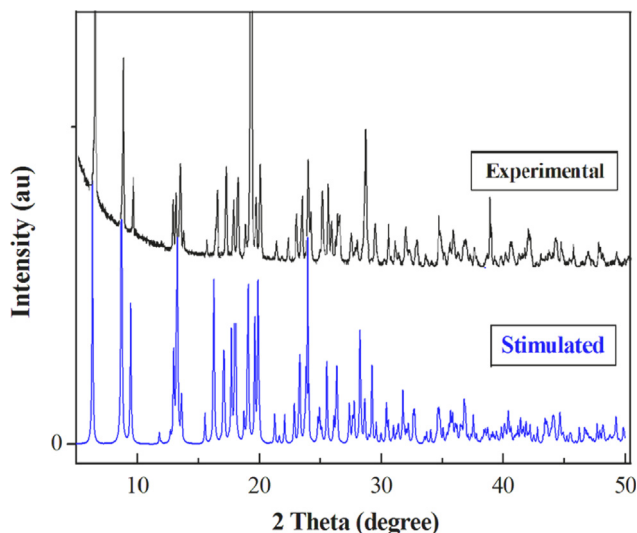


Fig. 4. Comparing the simulated XPRD pattern calculated from single-crystal structure and experimental ones for bulk sample of complex **1**.

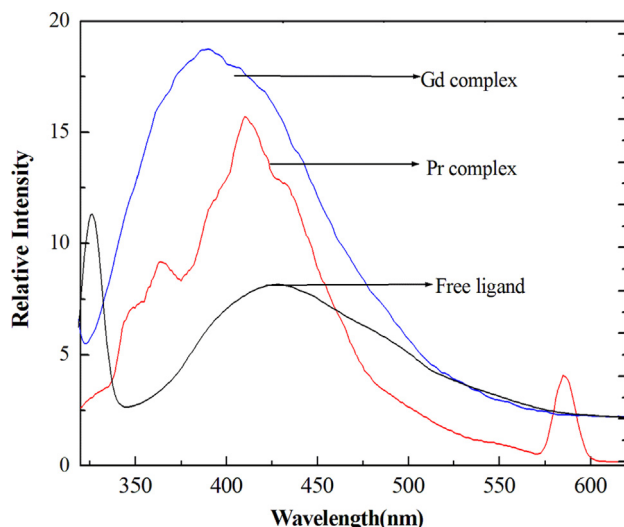


Fig. 5. Room-temperature solid-state photoluminescence spectra of Hdpp⁻ ligand as well as complexes **1** (Pr) and **3** (Gd).

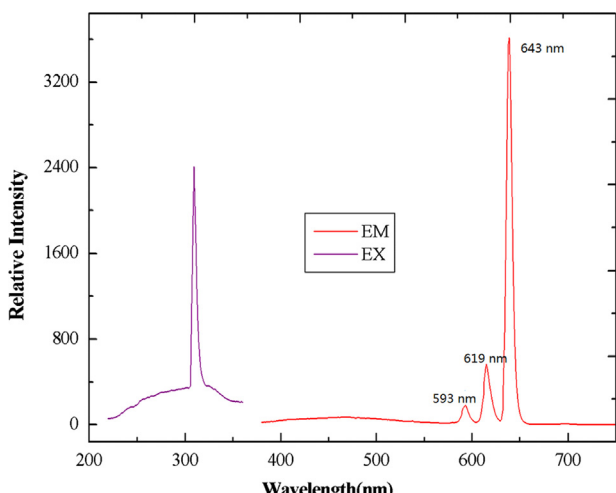


Fig. 6. Solid-state emission spectrum of the polymer **2** upon the excitation of $\lambda_{max}=307$ nm.

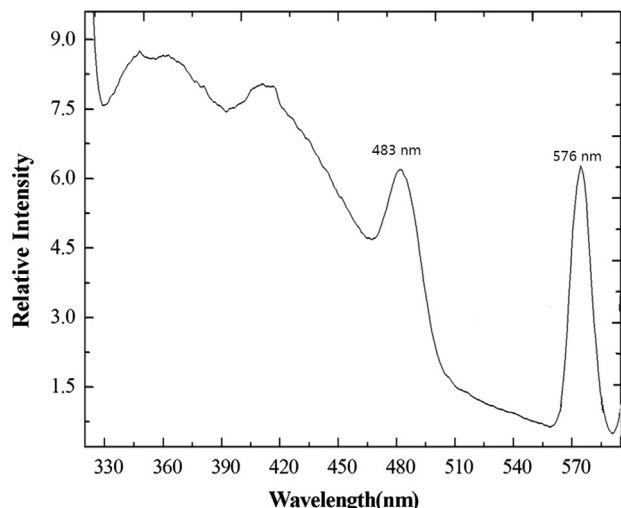


Fig. 7. Solid sample photoemission spectra of the complex **4** at room temperature.

The emission spectrum of complex **1** is composed of not only a narrow and sharp emission band between 360 and 380 nm (in ultraviolet region) with the maximum wavelength of 365 nm. The highest intense fluorescent emission band in blue region at $\lambda_{max}=415$ nm is corresponding to ${}^2P_{5/2} \rightarrow {}^8S_0$ transition for the Pr(III) ion [31]. By comparison of the other praseodymium based polymers, and the emission band with $\lambda_{max}=365$ nm is assigned to a ligand-centered (LC) fluorescence, based on the emission spectrum of free ligand [23]. The emission spectra of **3** exhibits a narrow fluorescent emission band at $\lambda_{max}=384$ nm, upon stimulated radiation with $\lambda_{max}=374$ nm, which corresponds to a ligand-centered (LC) fluorescence, as displayed in Fig. 5, and this is similar to the spectrum of gadolinium complex based on the amino acid-like ligands [24] and it is just a blue shift compared with the free ligand. The metal centered (MC) electronic levels of Gd(III) are known to be located at $31,000\text{ cm}^{-1}$, typically well above the ligand-centered electronic levels of aromatic ligands, therefore, ligand-to-metal energy transfer and the consequent MC luminescence cannot be observed. The maxima of compounds **1** and **3** are slightly blueshifted with respect to the free ligand, which is mainly due to an intraligand $\pi-\pi^*$ transition [25].

As reported in Fig. 6, excitation through the band $\lambda_{max}=307$ nm, the europium complex of **2** produces several sharp line emission spectra in the red region with the maximum wavelength of $\lambda_{max}=593$, 619, 643 nm, respectively. It displays intensity red luminescences and the characteristic $f-f$ transitions of a Eu(III) ion, the strong intensities of emissions at 593, 618 and 643 nm are attributed to ${}^5D_0 \rightarrow {}^7F_1$, ${}^5D_0 \rightarrow {}^7F_2$ and ${}^5D_0 \rightarrow {}^7F_3$ transitions, respectively.[26] The spectra is dominated by the intense of ${}^5D_0 \rightarrow {}^7F_2$ electron dipole transition, and the intensity ratio of ${}^5D_0 \rightarrow {}^7F_2$ / ${}^5D_0 \rightarrow {}^7F_1$ was 4.26, much higher than 0.67, a typical value for a centrosymmetric Eu(III) center. This high ratio therefore signifies that the Eu(III) ion adopts a noncentrosymmetric coordination environment [27,28], observed in the single crystal structure. It is noteworthy that the Eu(III) complex shows a higher intense fluorescence emission than that of the free N-heterocyclic dicarboxylic acid ligand [29], and very high Stokes shifts is observed.

The photoluminescence spectrum of **4** display medium strong solid-state emissions in blue-green-yellow region when excited at 331 nm, as depicted in Fig. 7. The emission bands at 483 and 576 nm indicate the characteristic behaviors of Dy(III) ions, which are assigned to ${}^4F_{9/2} \rightarrow {}^6H_J$ ($J=15/2$ and $13/2$) transitions, respectively. Moreover, the yellow hypersensitive transition ${}^4F_{9/2} \rightarrow {}^6H_{13/2}$, as the preferred transition for dysprosium-based luminescent materials, is more intense than the blue transition of ${}^4F_{9/2} \rightarrow {}^6H_{15/2}$.

This can be attributed to the noncentrosymmetric coordination environment around the Dy(III) centers, and also implies that H₂dpp ligand is suitable for sensitization of the yellow luminescence for Dy(III) ions [30,31]. From the emission spectra mentioned above, it can be found that the energy transfer from the organic ligands to Eu(III) is more effective than that to Dy(III), Gd(III) and Pr(III) ion [32].

3.4. Magnetic properties

Variable-temperature direct current magnetic susceptibility measurements were performed on micro-crystalline samples of complexes **1–5**. The results are illustrated in Figs. 8 and 9 and Fig. S10, Supplementary material, respectively. As depicted in Fig. 8, the $\chi_M T$ product of **1** at room temperature is $1.52 \text{ cm}^3 \text{ K mol}^{-1}$, which is somewhat lower than that expected value for a magnetically non-interacting Pr(III) compound ($1.58 \text{ cm}^3 \text{ mol}^{-1} \text{ K}$) in ${}^3\text{H}_4$ ground state ($g=4/5$) [33]. Upon cooling, the $\chi_M T$ value decreases with the measurement temperature and arrives at the minimum value ($0.019 \text{ cm}^3 \text{ K mol}^{-1}$) at 2 K. The magnetic susceptibilities of **1** beyond 40 K follow the modified Curie–Weiss law [$\chi_M = \chi_0 + C/(T - \theta)$] with $\chi_0 = -2.3 \times 10^{-2} \text{ cm}^3 \text{ mol}^{-1}$, Curie constant $C = 0.17 \text{ cm}^3 \text{ mol}^{-1} \text{ K}$, and Weiss constant $\theta = -2.47 \text{ K}$. There is no available expression to determine the magnetic susceptibilities of such 3D systems with large anisotropy [34]. As far as the existence of a strong spin–orbit coupling for Pr(III) atoms is concerned, the magnetic data were analyzed by the following approximate treatment equations previously derived by McPherson et al. [35]

$$\chi_{Pr} = \frac{Ng^2\beta^2}{k(T-\theta)(1+2e^{-x}+2e^{-4x}+2e^{-9x}+2e^{-16x})} \quad (1)$$

$$x = \lambda/kT \quad (2)$$

$$\chi_{total} = \frac{\chi_{Pr}}{1-(2zJ'/Ng^2\beta^2)\chi_{Pr}} \quad (3)$$

In this expression, N , β , k and g have their usual meanings, and λ is spin–orbit coupling parameter, and the Zeeman splitting was treated isotropically for the sake of simplicity [36]. The zJ' parameter based on the molecular field approximation in Eq. (3) is introduced to simulate the magnetic interaction between the Pr(III) ions. The best fit to the magnetic susceptibilities of **1** in the whole temperature range gave the parameters $\lambda = 1.47 \text{ cm}^{-1}$, $zJ' = -0.13 \text{ cm}^{-1}$, $g = 0.91$, $\theta = -1.59$ and $R = 1.7 \times 10^{-4}$ (R is the

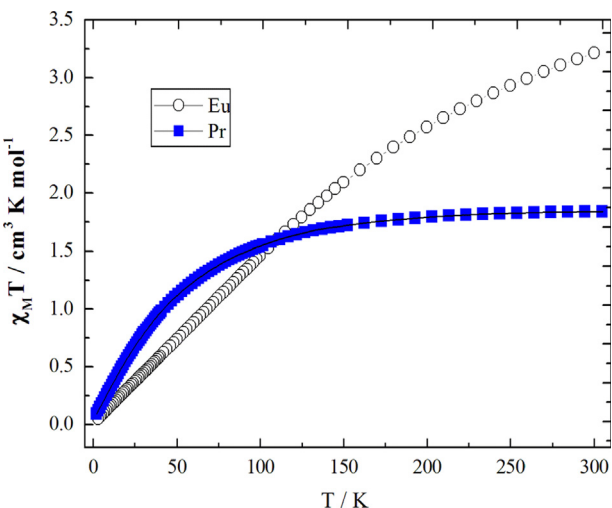


Fig. 8. Temperature dependence of $\chi_M T$ for **1** (○) and **2** (■) at 0.2 T between 2 and 300 K. The solid lines represent the theoretical values based on the corresponding equations.

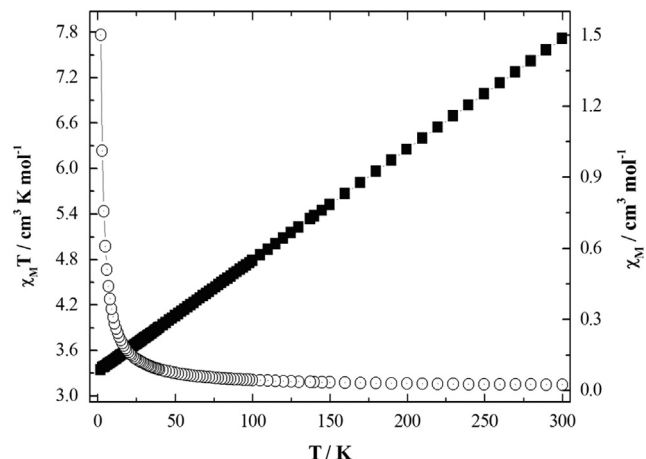


Fig. 9. Plot of χ_M (○) and $\chi_M T$ (■) versus T under a dc field of 0.2 T for **3**. The solid line is the best fit with the parameters in the text.

agreement factor defined as $R = \sum[(\chi_M)_{obs} - (\chi_M)_{cal}]^2 / \sum[(\chi_M)_{obs}]^2$. The absolute value of λ is slightly smaller than that reported in the compound of $[\text{Pr}_2(\text{C}_2\text{O}_4)_2(\text{pyc})_2(\text{H}_2\text{O})_2]_n$ [35](b). But antiferromagnetic coupling between adjacent Pr(III) ions could not be explicitly deduced from this result due to the existence of strong spin–orbit coupling for lanthanide atoms. The decrease in $\chi_M T$ possibly originates in the thermal depopulation of the highest Stark components deriving from the splitting of the free-ion ground state, ${}^3\text{H}_4$, by the crystal field [37].

A similar evolution is observed in the case of europium complex **2**. As illustrated in Fig. 8, at 300 K, the observed $\chi_M T$ is equal to $3.11 \text{ cm}^3 \text{ K mol}^{-1}$, which is slightly higher than the expected for thermal population of an excited state based on two isolated Eu(III) ions (theoretical value is $3.05 \text{ cm}^3 \text{ K mol}^{-1}$, $g = 3/2$) [38]. Upon cooling, this value decreases to reach value of $0.032 \text{ cm}^3 \text{ mol}^{-1} \text{ K}$ at 1.9 K. Such behavior can be referred to the thermal population of the Stark component ${}^7\text{F}_0$ ground state of free Eu(III) ions at very low temperature or the possible presence of a weak antiferromagnetic coupling between the Eu(III) ions mediated by the carboxylic group within the entire temperature range, or due to the presence of thermally populated excited states.

The temperature dependence of χ_M and $\chi_M T$ for **3** is displayed in Fig. 9, from which we can see $\chi_M T$ is equal to $7.84 \text{ cm}^3 \text{ K mol}^{-1}$ at 300 K, which is close to the value for an isolated Gd^{3+} ions (${}^8\text{S}_{7/2}$). When the temperature is lower, $\chi_M T$ decreases rapidly to $3.31 \text{ cm}^3 \text{ K mol}^{-1}$ at 2 K. Considering the $\text{Gd}^{(III)}$ ion has a ${}^8\text{S}_{7/2}$ ($L=0$) ground state configuration, which is spherically symmetric and is therefore not susceptible to crystal field effect [39], and the paramagnetism $\text{Gd}^{(III)}$ ion being in the 3D polymer, in which the two adjacent $\text{Gd}^{(III)}$ ions are double bridged through deprotonated carboxylic group from dpp^{2-} with the large $\text{Gd} \cdots \text{Gd}$ separation [40,41]. This allows us to consider that, crystal structure of **3** would behave as a uniform chain of $\text{Gd}^{(III)}$ ions, bridged by Heimda ligands, from a magnetic point of view (see Fig. 1a). Having this in mind and taking into account the large value of the local interacting spin [$S = 7/2$], the classical spin expression derived by Fisher to describe the magnetic behavior of a uniform chain with large spins Eq. (4) applies for **3** [43]. In this expression, u is the Langevin function defined as

$$\chi = \frac{Ng^2\beta^2}{3KT} S(S+1) \left[\frac{1+u}{1-u} \right] \quad (4)$$

$u = \coth[J(S+1)/KT] - KT/J(S+1)$ with N , β , k , and g have their usual meanings, and J is the exchange coupling parameter between adjacent spins. The best least squares fitting parameters

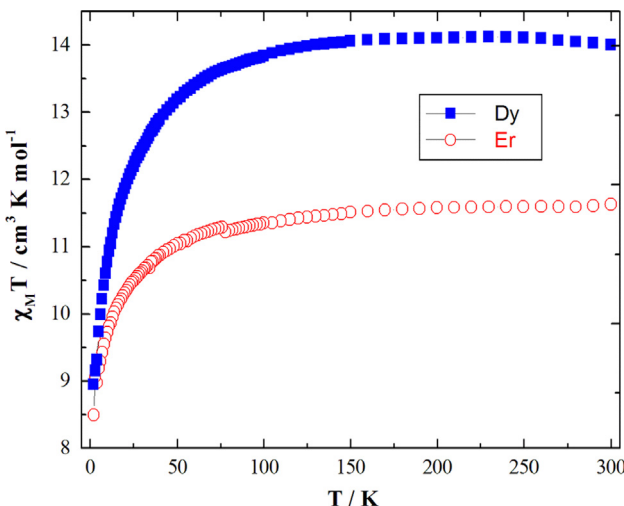


Fig. 10. Temperature dependence of the magnetic susceptibility in a 0.2 T field for **4** and **5**.

are $J = -0.032 \text{ cm}^{-1}$, $g = 2.01$ and $R = 1.46 \times 10^{-5}$ (R is the agreement factor defined as $R = \sum[(\chi_M)_{\text{obs}} - (\chi_M)_{\text{calc}}]^2 / \sum[(\chi_M)_{\text{obs}}]^2$). The result indicates that complex **3** exhibits a weak antiferromagnetic interaction between Gd(III) ions [42]. Moreover, we tried to fit the reciprocal molar magnetic susceptibilities of **3** as a function in whole temperature range with Curie–Weiss law, $\chi = C/(T-\theta)$, and found it closely followed the Curie–Weiss law, resulting in $C = 7.13 \text{ emu mol}^{-1} \text{ K}$ and $\theta = -2.36 \text{ K}$ with $R = 1.24 \times 10^{-5}$, as reported in Fig. S10, Supplementary material. The small negative θ value further supports the presence of very weak antiferromagnetic interactions between Gd^{3+} ions. The reason for the small J value results from the fact that the large Gd(III)...Gd(III) separation and 4f electrons are influenced very little by the surrounding environment, and unpaired electrons around Gd^{3+} are very difficult to transfer to the 5d or 6s orbital [44]. It is also found that with temperature lowering, $\chi_M T$ product of **3** decreases more abrupt than those of complexes **1** and **2**.

Complexes **4** and **5** displayed magnetic behaviors which are different from those of the complexes **1–3**. As illustrated in Fig. 10, for dysprosium complex of **4**, $\chi_M T$ product at room temperature is equal to $13.82 \text{ cm}^3 \text{ K mol}^{-1}$, which is nearly consistent with the expected value of $14.2 \text{ cm}^3 \text{ K mol}^{-1}$ for isolated Dy(III) ion (${}^6\text{H}_{15/2}$, $S=5/2$, $L=5$, $g=4/3$) [45]. When the temperature is lowered, $\chi_M T$ value decrease slightly slowly down to $13.27 \text{ cm}^3 \text{ K mol}^{-1}$ at 50 K. Below 50 K, $\chi_M T$ decreases rapidly with cooling up to a minimum of $8.62 \text{ cm}^3 \text{ K mol}^{-1}$ at the lowest temperature 2 K. The abrupt decrease of $\chi_M T$ at low temperature could be due to the possible antiferromagnetic interaction between $\text{Ln}(\text{III})$ ions or the field saturation effect. [46].

For Er(III) compound **5**, the $\chi_M T$ value is equal to $11.62 \text{ cm}^3 \text{ mol}^{-1} \text{ K}$ at 300 K, which is close to the expected $11.48 \text{ cm}^3 \text{ K mol}^{-1}$ for one isolated Er(III) ion (ground state ${}^4\text{I}_{15/2}$, $S=3/2$, $L=6$, $J=15/2$ and $g=6/5$) [47]. Lowering the temperature caused a gradually descend in $\chi_M T$ product from 300 to 50 K, then decreases quickly to $8.04 \text{ cm}^3 \text{ K mol}^{-1}$ at 2 K, which could arise from a selective depopulation of the excited crystal field state and antiferromagnetic interaction between Er(III) ions [48,35](a).

In this series of complexes, although they nearly have the similar structure, magnetic studies revealed that the Dy(III) **4** complex and Er(III) complex **5** are nearly paramagnet at higher temperature, whereas the Gd(III) complex **3** obviously shows antiferromagnetic coupling between lanthanide ions, while the depopulation of the Stark levels or possibly antiferromagnetic coupling dominates the magnetic properties of complexes **1** and **2**.

4. Conclusions

Reactions of the multi-donor dicarboxylate ligand with lanthanide (III) nitrates afford a new family of lanthanide organic frameworks containing mixed donor ligand. These results suggest that the structural characteristic of organic linker play an important role in governing the final networks. The luminescence emission spectra of the complexes vary depending on which lanthanide (III) ion is present. The complexes **2** and **4**, display a strong characteristic emission in visible region. Informative susceptibility studies indicate that their magnetic properties are essential difference, though the magnetic centers mediated through the same carboxylic bridging.

Supplementary material

CCDC 913454–913458–913458 contain the supplementary crystallographic data for complexes in this paper. These data can be obtained free of charge from the Cambridge Crystallographic Data Centre via www.ccdc.cam.ac.uk/data_request/cif, or e-mail to: deposit@ccdc.cam.ac.uk. Supplementary data associated with this article, can be found, in the online version, <http://dx.doi.org/10.1016/j.jssc.2013.xxxxx>.

Acknowledgments

We gratefully acknowledge financial support of this work by the National Natural Science Foundation of China (Nos. 21071074, 21271098 and 21273101), the Foundation of the Back-bone Teachers in Universities of Henan Province, China (No. 2012GGJS158) and the National innovative entrepreneurship training program in China University (No. 201210482014) and Ministry of Higher Education of Malaysia (Grant No. UM.C/HIR-MOHE/SC/03).

Appendix A. Supporting information

Supplementary data associated with this article can be found in the online version at <http://dx.doi.org/10.1016/j.jssc.2013.08.029>.

References

- [1] (a) S.J.A. Pope, B.J. Coe, S. Faulkner, E.V. Bichenkova, X. Yu, K.T. Douglas, *J. Am. Chem. Soc.* 126 (2004) 9490;
 (b) H.W. Hou, G. Li, L.K. Li, Y. Zhu, X.R. Meng, Y.T. Fan, *Inorg. Chem.* 42 (2003) 428;
 (c) B. Zhao, X.Y. Chen, Z. Chen, W. Shi, P. Cheng, S.P. Yan, D.Z. Liao, *Chem. Commun.* (2009) 3113;
 (d) D. Maspoch, D. Ruiz-Molina, J. Veciana, *Chem. Soc. Rev.* 36 (2007) 770;
 (e) P. Mahata, A. Sundaresan, S. Natarajan, *Chem. Commun.* (2007) 4471;
 (f) M.L. Cable, J.P. Kirby, K. Sorasaenee, H.B. Gray, A. Ponce, *J. Am. Chem. Soc.* 129 (2007) 1474;
 (g) A.L. Cheng, Y. Ma, J.Y. Zhang, E.Q. Gao, *Dalton Trans.* (2008) 1993;
 (h) N. Klein, I. Senkovska, K. Gedrich, U. Stoeck, A. Henschel, U. Mueller, S. Kaskel, *Angew. Chem. Int. Ed.* 48 (2009) 9954.
- [2] (a) Z.H. Zhang, Y. Song, T. Okamura, Y. Hasegawa, W.Y. Sun, N. Ueyama, *Inorg. Chem.* 45 (2006) 2896;
 (b) J. Xia, B. Zhao, H.S. Wang, W. Shi, Y. Ma, H.B. Song, P. Cheng, *Inorg. Chem.* 46 (2007) 3450;
 (c) E.G. Moore, G. Szigethy, J. Xu, L.O. Pálsson, A. Beeby, K.N. Raymond, *Angew. Chem. Int. Ed.* 47 (2008) 9500;
 (d) C. Piguet, E.R. Minten, G.J.C. Bernardinelli, G. Bünzli, G. Hopfgartner, *J. Chem. Soc. Dalton Trans.* (1997) 421;
 (e) S.H. Jhung, J.H. Lee, J.W. Yoon, C. Serre, G. Ferey, J.S. Chang, *Adv. Mater.* 19 (2007) 121.
- [3] (a) P.F. Shi, B. Zhao, G. Xiong, Y.L. Hou, P. Cheng, *Chem. Commun.* 48 (2012) 8231;
 (b) S.V. Eliseeva, J.C.G. Bünzli, *Chem. Soc. Rev.* 39 (2010) 189;
 (c) N.S. Baek, Y.H. Kim, Y.K. Eom, J.H. Oh, H.K. Kim, A. Aebsicher, F. Gumy, A.S. Chauvin, J.C.G. Bünzli, *Dalton Trans.* 39 (2010) 1532.
- [4] (a) Q.L. Zhu, T.L. Sheng, R.B. Fu, S.M. Hu, J.S. Chen, S.C. Xiang, C.J. Shen, X.T. Wu, *Cryst. Growth Des.* 12 (2009) 5128;

- (b) M.D. Allendorf, C.A. Bauer, R.K. Bhakta, R.J.T. Houk, *Chem. Soc. Rev.* 38 (2009) 1330;
- (c) M. Montalti, L. Prodi, N. Zaccheroni, L. Charbonniere, L. Douce, R. Ziessel, *J. Am. Chem. Soc.* 123 (2001) 12694.
- [5] (a) R. Cao, D.F. Sun, Y.C. Liang, M.C. Hong, K. Tatsumi, Q. Shi, *Inorg. Chem.* 41 (2002) 2087;
- (b) D. Ghoshal, T.K. Maji, G. Mostafa, S. Sain, T.H. Lu, J. Ribas, E. Zangrandi, N. R. Chaudhuri, *J. Chem. Soc. Dalton Trans.* (2004) 1687;
- (c) S.N. Wang, H. Xing, J.F. Bai, Y.-Z. Li, Y. Pan, M. Scheer, X.Z. You, *Chem. Commun.* (2007) 2293;
- (d) S.N. Wang, J.F. Bai, Y.Z. Li, Y. Pan, M. Scheer, X.Z. You, *CrystEngComm* 9 (2007) 1084;
- (e) S.N. Wang, H. Xing, J.F. Bai, Y.Z. Li, Y. Pan, M. Scheer, X.Z. You, *Cryst. Growth Des.* 7 (2007) 747;
- (f) X.L. Sun, Z.J. Wang, S.Q. Zang, W.C. Song, C.X. Du, *Cryst. Growth Des.* 12 (2012) 4431;
- (g) B.L. Chen, L.B. Wang, Y.Q. Xiao, F.R. Fronczek, M. Xue, Y.J. Cui, G.D. Qian, *Angew. Chem. Int. Ed.* 48 (2009) 500.
- [6] (a) Y.G. Huang, F.L. Jiang, D.Q. Yuan, M.Y. Wu, Q. Gao, W. Wei, M.C. Hong, *Cryst. Growth Des.* 8 (2008) 167;
- (b) D. Min, S.W. Lee, *Inorg. Chem. Commun.* 5 (2002) 978;
- (c) P. Wang, J.P. Ma, Y.-B. Dong, R.Q. Huang, *J. Am. Chem. Soc.* 129 (2007) 10620;
- (d) L.F. Ma, B. Liu, L.Y. Wang, C.P. Li, M. Du, *Dalton Trans.* 39 (2010) 2301;
- (e) A. White, D.A. Chengelis, K.A. Gogick, J. Stehman, N.L. Rosi, S. Petoud, *J. Am. Chem. Soc.* 131 (2009) 18069.
- [7] (a) Z.M. Wang, B. Zhang, H. Fujiwara, H. Kobayashi, M. Kurmoo, *Chem. Commun.* (2004) 416;
- (b) J.L. Manson, J.G. Lecher, J.-Y. Gu, U. Geiser, J.A. Schlueter, R. Henning, X.P. Wang, A.J. Schultz, H.J. Koo, M.H. Whangbo, *J. Chem. Soc. Dalton Trans.* (2003) 2905;
- (c) Z. Chen, B. Zhao, P. Cheng, X.Q. Zhao, W. Shi, Y. Song, *Inorg. Chem.* 48 (2009) 3493.
- [8] (a) M. Vierthaus, H. Henke, C.E. Anson, A.K. Powell, *J. Eur. Inorg. Chem.* (2003) 2283;
- (c) H. Kageyama, D.I. Khomskii, R.Z. Levitin, A.N. Vasil'ev, *Phys. Rev. B* 67 (2003) 224422;
- (d) P. Radhakrishnatt, B. Gillon, G. Chevrierts, *J. Phys.: Condens. Matter* 5 (1993) 6147;
- (e) J.P. Costes, F. Dahan, A. Dupuis, J.P. Laurent, *New J. Chem.* 22 (1998) 1525;
- (f) X.X. Hu, C.L. Pan, J.Q. Xu, X.B. Cui, G.D. Yang, T.G. Wang, *Eur. J. Inorg. Chem.* 43 (2004) 1566;
- (g) X.Y. Wang, H.Y. Wei, Z.M. Wang, Z.D. Chen, *Inorg. Chem.* 44 (2005) 572.
- [9] (a) F.M. Tabellion, S.R. Seidel, A.M. Arif, P.J. Stang, *Angew. Chem. Int. Ed.* 40 (2001) 1529;
- (b) L. Pan, E.B. Woodlock, X. Wang, K.C. Lam, A.L. Rheingold, *Chem. Commun.* (2001) 1762;
- (c) M.L. Tong, Y.M. Wu, J. Ru, X.M. Chen, H.C. Chang, S. Kitagawa, *Inorg. Chem.* 41 (2002) 4846;
- (d) W.J. Zhuang, X.J. Zheng, L.C. Li, D.Z. Liao, H. Ma, L.P. Jin, *CrystEngComm* 9 (2007) 653;
- (e) C.B. Aakeroy, J. Desper, J.F. Urbina, *CrystEngComm* 7 (2005) 193;
- (f) Z.Z. Lin, F.L. Jiang, D.Q. Yuan, L. Chen, Y.F. Zhou, M.C. Hong, *Eur. J. Inorg. Chem.* (2005) 1927;
- (g) G. Chen, J. Wu, Q.J. Lu, H.R.H. Gutierrez, Q. Xiong, M.E. Pellen, J.S. Petko, D.H. Werner, P.C. Eklund, *Nano Lett.* 8 (2008) 1341;
- (h) A. Sonnauer, C. Näther, H.A. Höppe, J. Senker, N. Stock, *Inorg. Chem.* 46 (2007) 9968.
- [10] (a) T.H. Zhou, F.Y. Yi, P.X. Li, J.G. Mao, *Inorg. Chem.* 49 (2010) 905;
- (b) T. Kajiwara, M. Hasegawa, A. Ishii, K. Katagiri, M. Baatar, S. Takaishi, N. Iki, M. Yamashita, *Eur. J. Inorg. Chem.* 36 (2008) 5565;
- (c) G.F. Xu, Q.L. Wang, P. Gamez, Y. Ma, R. Cle'rac, de, J.K. Tang, S.P. Yan, P. Cheng, D.Z. Liao, *Chem. Commun.* 46 (2010) 1506.
- [11] (a) G.M. Sheldrick, *SHELXS 97, Program for the Solution of Crystal Structure, University of Göttingen, Germany*, 1997;
- (b) G.M. Sheldrick, *SHELXL 97, Program for the Crystal Structure Refinement, University of Göttingen, Germany*, 1997.
- [12] K.L. Wong, G.L. Law, Y.Y. Yang, W.T. Wong, *Adv. Mater.* 18 (2006) 1051.
- [13] R. Baggio, M.T. Garland, O. Pen-a, M. Perez, *Inorg. Chim. Acta* 358 (2005) 2332.
- [14] R. Shy尼, S. Biju, M.L.P. Reddy, Alan H. Cowley, M. Findlater, *Inorg. Chem.* 46 (2007) 11025.
- [15] (a) C.Y. Wang, Z.M. Wilseck, R.M. Supkowski, R.L. LaDuca, *CrystEngComm* 13 (2011) 1391;
- (b) L. Carlucci, G. Ciani, D.M. Proserpio, *Cryst. Growth Des.* 5 (2005) 37;
- (c) S. Natarajan, P. Mahata, *Chem. Soc. Rev.* 38 (2009) 2304;
- (d) L. Cheng, L.M. Zhang, Q.N. Cao, S.H. Gou, X.Y. Zhang, L. Fang, *Cryst. Eng. Comm.* 14 (2012) 7502;
- (f) M. Sarkar, K. Biradha, *Chem. Commun.* (2005) 2229.
- [16] (a) S.Q. Zang, R. Liang, Y.-J. Fan, H.W. Hou, T.C.W. Mak, *Dalton Trans.* 39 (2010) 8022;
- (b) X.L. Sun, W.C. Song, S.Q. Zang, C.X. Du, H.W. Hou, Thomas C.W. Mak, *Chem. Commun.* 48 (2012) 2113;
- (c) M.S. Liu, Q.Y. Yu, Y.P. Cai, C.Y. Su, X.M. Lin, X.X. Zhou, J.W. Cai, *Cryst. Growth Des.* 8 (2008) 4083.
- [17] R. Feng, L. Chen, Q.-H. Chen, X.-C. Shan, Y.-L. Gai, F.-L. Jiang, M.C. Hong, *Cryst. Growth Des.* 11 (2011) 1705.
- [18] (a) S. Chen, R.Q. Fan, C.F. Sun, P. Wang, Y.L. Yang, Q. Su, Y. Mu, *Cryst. Growth Des.* 12 (2012) 1337;
- (b) S.L. Zheng, M.-L. Tong, X.M. Chen, *Coord. Chem. Rev.* 246 (2003) 185;
- (c) S.R. Batten, K.S. Murray, *Coord. Chem. Rev.* 246 (2003) 103;
- (d) S.R. Batten, S.M. Neville, D.R. Turner, *Coordination Polymers: Design, Analysis and Application*, Royal Society of Chemistry, Cambridge (2008) 07.
- [19] (a) Y.Y. Zhu, Z.G. Sun, H. Chen, J. Zhang, Y. Zhao, N. Zhang, L. Liu, X. Lu, W.-N. Wang, F. Tong, L.C. Zhang, *Cryst. Growth Des.* 9 (2009) 3228;
- (b) J.L. Song, J.-G. Mao, *Chem. -Eur. J.* 11 (2005) 1417;
- (c) X.J. Zhang, Y.H. Xing, J. Han, X.Q. Zeng, M.F. Ge, S.-Y. Niu, *Cryst. Growth Des.* 8 (2008) 3680;
- (d) Y. Li, F.-K. Zheng, X. Liu, W.-Q. Zou, G.-C. Guo, C.-Z. Lu, J.-S. Huang, *Inorg. Chem.* 45 (2006) 6308;
- (e) Z.H. Weng, D.C. Liu, Z.L. Chen, H.H. Zou, S.N. Qin, F.P. Liang, *Cryst. Growth Des.* 9 (2009) 4163.
- [20] (a) A. Fratini, G. Richards, E. Larder, S.S. wavey, *Inorg. Chem.* 47 (2008) 1030;
- (b) A. Fratini, S. Swavey, *Inorg. Chem. Commun.* 10 (2007) 636;
- (c) Z.H. Zhang, T.A. Okamura, Y. Hasegawa, H. Kawaguchi, L.Y. Kong, W.Y. Sun, N. Ueyama, *Inorg. Chem.* 44 (2005) 6219.
- [21] M.A. Braverman, R.M. Supkowski, R.L. LaDuca, *J. Solid State Chem.* 180 (2007) 1852.
- [22] (a) Z. Miskolczy, L. Biczók, I. Jablonkai, *J. Phys. Chem. A* 116 (2012) 899;
- (b) T.L. Esplin, M.L. Cable, H.B. Gray, A. Ponce, *Inorg. Chem.* 49 (2010) 4643.
- [23] Y.L. Huang, M.Y. Huang, T.H. Chan, B.C. Chang, K.H. Lii, *Chem. Mater.* 19 (2007) 3232.
- [24] (a) X.M. Jing, H. Meng, G.H. Li, Y. Yu, Q.S. Huo, M. Eddaoudi, Y.L. Liu, *Cryst. Growth Des.* 10 (2010) 3489;
- (b) S.Q. Zhang, F.L. Jiang, M.Y. Wu, R. Feng, J. Ma, W.T. Xu, M.C. Hong, *Inorg. Chem. Commun.* 14 (2011) 1400.
- [25] (a) Y.Q. Sun, J. Zhang, Y.M. Chen, G.Y. Yang, *Angew. Chem. Int. Ed.* 44 (2005) 5814;
- (b) K.A. Thiakou, V. Nastopoulos, A. Terzis, C.P. Raptopoulou, S.P. Perlepes, *Polyhedron* 25 (2006) 539.
- [26] (a) W.T. Chen, Q.Y. Luo, D.S. Liu, H.L. Chen, Y.P. Xu, *Inorg. Chem. Commun.* 11 (2008) 899;
- (b) C.X. Wang, C.X. Du, Y.H. Li, Y.J. Wu, *Inorg. Chem. Commun.* 8 (2005) 379;
- (c) Z.F. Li, J.B. Yu, L. Zhou, H.J. Zhang, R.P. Deng, Z.Y. Guo, *Org. Electron.* 9 (2008) 487.
- [27] H. Zhu, Z.M. Wang, S. Gao, *Inorg. Chem.* 46 (2007) 1337.
- [28] (a) R. Martínez-Máñez, F. Sancenón, *Chem. Rev.* 103 (2003) 4419;
- (b) X. Feng, L.Y. Wang, J.S. Zhao, J.G. Wang, S.W. Ng, B. Liu, X.G. Shi, *CrystEngComm* 12 (2010) 774.
- [29] (a) K.A. Thiakou, V. Nastopoulos, A. Terzis, C.P. Raptopoulou, S.P. Perlepes, *Polyhedron* 25 (2006) 539;
- (b) X.F. Li, T.F. Liu, Q.P. Lin, R. Cao, *Cryst. Growth Des.* 10 (2010) 608.
- [30] W.P.W. Lai, W.T. Wong, B.K.F. Lic, K.W. Cheah, *New J. Chem.* 26 (2002) 576.
- [31] (a) J.M. Calderon Moreno, V.G. Pol, S.H. Suh, M. Popa, *Inorg. Chem.* 49 (2010) 10067;
- (b) J. Scholten, G.A. Rosser, J. Wahsner, N. Alzakhem, C. Bischof, F. Stog, A. Beeby, M. Seitz, J. Am. Chem. Soc. 134 (2012) 13915.
- [32] (a) R. Martínez-Máñez, F. Sancenón, *Chem. Rev.* 103 (2003) 4419;
- (b) C. Janiak, *Dalton Trans.* (2003) 2781;
- (c) C. Seward, N.X. Hu, S. Wang, *J. Chem. Soc. Dalton Trans.* (2001) 134;
- (d) A.L. Cheng, N. Liu, Y.F. Yue, Y.W. Jiang, E.-Q. Gao, C.H. Yan, M.Y. He, *Chem. Commun.* (2007) 407;
- (e) J. Cepeda, R. Balda, G. Beobide, O. Castillo, J. Fernández, A. Luque, S. Pérez-Yáñez, P. Román, *Inorg. Chem.* 51 (2012) 7875.
- [33] M. Hernández-Molina, P.A. Lorenzo-Luis, T. LoÁpez, C. Ruiz-Pérez, F. Lloret, M. Julve, *CrystEngComm* 31 (2000) 1.
- [34] (a) K.A. White, D.A. Chengelis, M. Zeller, S.J. Geib, J. Szakos, S. Petoud, N.L. Rosi, *Chem. Commun.* (2009) 4506;
- (b) N. Xu, W. Shi, D.Z. Liao, S.P. Yan, P. Cheng., *Inorg. Chem.* 47 (2008) 8748.
- [35] (a) I.A. Kahwa, J. Selbin, C.J. Oconnor, J.W. Foise, G.L. McPherson, *Inorg. Chim. Acta* 148 (1988) 265;
- (b) B. Li, W. Gu, L.Z. Zhang, J. Qu, Z.P. Ma, X. Liu, D.Z. Liao, *Inorg. Chem.* 45 (2006) 10425.
- [36] (a) Y.-S. Song, B. Yan, *Inorg. Chim. Acta* 358 (2005) 191;
- (b) Z.F. Li, J.B. Yu, L. Zhou, H.J. Zhang, R.P. Deng, *Inorg. Chem. Commun.* 11 (2008) 1284;
- (c) Y. Huang, Y.S. Song, B. Yan, M. Shao, *J. Solid State Chem.* 181 (2008) 1731.
- [37] (a) D. Aguil, L.A. Barrios, F. Luis, A. Repolles, O. Roubeau, S.J. Teat, G. Aromi, *Inorg. Chem.* 49 (2010) 6784;
- (b) X.J. Wang, Z.-M. Cen, Q.L. Ni, X.F. Jiang, H.-C. Lian, L.-C. Gui, H.-H. Zuo, Z. Y. Wang, *Cryst. Growth Des.* 10 (2010) 2960.
- [38] (a) S. Chandra Manna, E. Zangrandi, A. Bencini, C. Benelli, N.R. Chaudhuri, *Inorg. Chem.* 45 (2006) 9114;
- (b) T. Zhou, F.Y. Yi, P.X. Li, J.G. Mao, *Inorg. Chem.* 49 (2010) 905;
- (c) N. Ishikawa, T. Iino, Y. Kaizu, *J. Phys. Chem. A* 106 (2002) 9543.
- [39] (a) M. Andruh, E. Bakalbassis, O. Kahn, J. Christian Trombe, P. Porchers, *Inorg. Chem.* 32 (1993) 1616;
- (b) M.H. Molina, C.R. Pérez, T. López, F. Lloret, M. Julve, *Inorg. Chem.* 42 (2003) 5456;
- (c) M.E. Fisher, *Am. J. Phys.* 32 (1964) 343.
- [40] (a) O. Kahn, *Molecular Magnetism*, VCH Publishers, New York, 1993;
- (b) J.-P. Costes, J.M. Clemente-Juan, F. Dahan, F. Nicodème, M. Verelst, *Angew.*

- Chem. Int. Ed. 41 (2002) 323;
(c) L.E. Roy, T. Hughbanks, J. Am. Chem. Soc. 128 (2006) 568.
- [41] (a) W. Plass, G. Fries, Z. Anorg. Allg. Chem. 623 (1997) 1205;
(b) A. Panagiotopoulos, T.F. Zafiropoulos, P. Spyros, E. Perlepes, I. Bakalbassis, O. Masson-Ramade, A. Kahn, Terzis, C.P. Raptopoulou, Inorg. Chem. 34 (1995) 4918;
(c) S.T. Hastcher, W. Urland, Angew. Chem. Int. Ed. 42 (2003) 2862.
- [42] (a) Z.B. Han, G.X. Zhang, M.H. Zeng, C.H. Ge, X.H. Zou, G.X. Han, CrystEngComm 11 (2009) 2629;
(b) J.-P. Costes, J.M. Clemente- Juan, F. Dahan, F. Nicodème, Dalton Trans. (2003) 1272;
(c) L. Cañadillas-Delgado, O. Fabelo, J. Cano, J. Pasán, F.S. Delgado, F. Lloret, M. Julve, C. Ruiz-Pérez, CrystEngComm 11 (2009) 2131.
- [43] (a) M.E. Fisher, Am. J. Phys. 32 (1964) 343;
(b) L. Cañadillas-Delgado, J. Pasández- Molina, O. Fabelo, M. Hernández- Molina, F. Lloret, M. Julve, C. Ruiz-Pérez, Inorg. Chem. 45 (2006) 10585.
- [44] M.L. Sun, J. Zhang, Q.P. Lin, P.X. Yin, Y.G. Yao, Inorg. Chem. 49 (2010) 9257.
- [45] (a) X.D. Guo, G.S. Zhu, Z.Y. Li, F.X. Sun, Z.H. Yang, S.L. Qiu, Chem. Commun. (2006) 3172;
- (b) P.H. Lin, T.J. Burchell, L. Ungur, L.F. Chibotaru, W. Wernsdorfer, M. Murugesu, Angew. Chem. Int. Ed. 48 (2009) 9489.
- [46] (a) L. Zhao, S.F. Xue, J.K Tang, Inorg. Chem. 51 (2012) 5994;
(b) N. Ishikawa, T. Iino, Y. Kaizu, J. Am. Chem. Soc. 124 (2002) 11440;
(c) P.C.R.S. Santos, H.I.S. Nogueira, F.A.A. Paz, R.A.S. Ferreira, L.D. Carlos, J. Klinowski, T. Trindade, Eur. J. Inorg. Chem. 19 (2003) 3609.
- [47] (a) P.-H. Lin, T.J. Burchell, R. Clerac, M. Murugesu, Angew. Chem. Int. Ed. 47 (2008) 8848;
(b) Y.N. Guo, X.H. Chen, S. Xue, J. Tang, Inorg. Chem. 50 (2011) 9705;
(c) C. Benelli, D. Gatteschi, Chem. Rev. 102 (2002) 2369.
- [48] (a) M.Y. Li, B. Liu, B.W. Wang, Z.M. Wang, S. Gao, M. Kurmoo, Dalton Trans. 40 (2011) 6038;
(b) N. Ishikawa, Y. Mizuno, S. Takamatsu, T. Ishikawa, S.-Y. Koshibara, Inorg. Chem. 47 (2008) 10217;
(c) M.A. Aldamen, J.M. Clemente-Juan, E. Coronado, C. Martí-Gastaldo, A. Gaita-Ariño, J. Am. Chem. Soc. 130 (2008) 8874;
(e) M. Sugita, N. Ishikawa, T. Ishikawa, S.-y. Koshibara, Y. Kaizu, Inorg. Chem. 45 (2006) 1299.